RIJKSINSTITUUT VOOR VOLKSGEZONDHEID EN MILIEU
NATIONAL INSTITUTE OF PUBLIC HEALTH AND THE ENVIRONMENT

RIVM report 481508009

Modelling land degradation in IMAGE 2

R.M. Hootsmans[1], A.F. Bouwman, R. Leemans
and G.J.J. Kreileman

April 2001

[1] Currently at Provincie Noord-Brabant, Bureau Beleidsinformatie en Cartografie (BiC)
Postbus 90151, 5200 MC 's-Hertogenbosch

This study was commissioned by the UN Environment Programme (UNEP), The Dutch National Research Programme on Global Air Pollution and Climate Change and The Netherlands' Ministry of Housing, Spatial Planning and the Environment.

RIVM, P.O. Box 1, 3720 BA Bilthoven, The Netherlands, telephone: 31-30-2743635; telefax: 31-30-2744435

National Institute for Public Health and the Environment
P.O. Box 1
3720 BA Bilthoven, The Netherlands
Telephone: 31 30 274 3377
Telefax: 31 30 2744435
E-mail: image-info@rivm.nl

Abstract

Food security may be threatened by loss of soil productivity as a result of human-induced land degradation. Water erosion is the most important cause of land degradation, and its effects are irreversible. This report describes the IMAGE land degradation model developed for describing current and future global problems of water erosion at a 0.5 by 0.5 degree longitude and latitude resolution. The sensitivity to water erosion is computed from the terrain erodibility (based on soil and terrain characteristics), rainfall erosivity and land cover. Sensitivity is expressed in relative terms. The results can be used to identify regions where problems of water erosion may present under scenarios of population and economic growth, technological change and climate change.

Abstract

Achteruitgang van de kwaliteit van land voor landbouwproductie als gevolg van land degradatie kan een bedreiging vormen voor de voedselproductie. Erosie veroorzaakt door oppervlakkige afstroming van neerslag is wereldwijd de belangrijkste vorm van land degradatie, met irreversibele effecten. Dit rapport beschrijft het IMAGE land degradatie model waarmee huidige en toekomstige problemen van erosie door regenval kunnen worden beschreven met een ruimtelijke resolutie van 0.5 breedtegraad bij 0.5 lengtegraad. De gevoeligheid voor water erosie wordt berekend uit een aantal bodemhoedanigheden en reliëf, de intensiteit van regenval en de landbedekking. De relatieve gevoeligheid voor water erosie wordt uitgedrukt in een kwalitatieve index, omdat kwantificering van bodemverlies op de gewasproductiviteit van land op mondiale schaal niet mogelijk is. De resultaten kunnen worden gebruikt om gebieden te identificeren waar problemen van erosie op kunnen treden, op basis van scenario's van groeiende bevolking en economie, technologische vooruitgang en klimaatverandering.

Foreword

The second meeting of the IMAGE advisory Board concluded that land degradation could strongly influence crop productivity and thus forms an important land-use driver to be included in the calculations of the Terrestrial Environment System of the IMAGE model. The Global Environmental Outlook project of UNEP also became strongly interested in more comprehensively assessing the future global impacts of land degradation. Together with the Dutch National Research Programme on Global Air Pollution and Climate Change, UNEP provided funding for the development of the methodology for the assessment of land degradation and case studies by the International Soil Reference and Information Centre (ISRIC), and the development of the IMAGE Land Degradation model described in this report.

The research would not have been possible without the long and detailed discussions with Jan Bakkes (RIVM), Niels Batjes and Vincent Van Engelen (ISRIC), Bert-Jan Heij (NRP), Miriam Schomakers (UNEP). The project was led by Gert Jan van den Born in an early phase. We appreciate that he convened all the useful contacts and conceptualized the first versions of the model. Finally we are grateful to ISRIC, which was instrumental in making the GLASOD and WISE data available to us and assisting in the creation of our generic model from their much more detailed assessments. Without their help, this project would have been much less successful.

Contents

Summary

Food security may be threatened by loss of soil productivity as a result of human-induced land degradation. Water erosion is the most important cause of land degradation, and its effects are irreversible. This report describes a land-degradation model to compute the land's sensitivity to water erosion in a qualitative sense. A qualitative approach is most appropriate, because it is impossible to estimate soil loss rates and effects on plant productivity for different water erosion processes at the scale of the IMAGE model (0.5 degree longitude by 0.5 degree latitude).

A modified version of the Universal Soil Loss Equation (USLE) (Wischmeier and Smith, 1978) was used. USLE was developed for the eastern part of the USA to compute soil loss by rainfall from agricultural land, using regression equations based on local data for rainfall, soil and terrain characteristics, vegetation and management practices.

Application of the USLE at a global scale requires modification on the basis of the scale and the availability of data on climate, terrain characteristics and land management. The simplified formulation of USLE is as follows:

$$E = f(T, R, V) \quad (1)$$

with: E - erosion hazard
T - terrain erodibility index (considering slope and soil type)
R - rainfall erosivity index
V - land use/cover index

The terrain erodibility index is composed of the soil erodibility index and relief index. The rating of soil characteristics is referred to as soil erodibility, based on soil texture and soil depth. The relief index is a landform characterization derived from a digital elevation model (based on differences in elevation within grid cells).

The calculation of the rainfall erosivity is based on the maximum mean monthly rainfall intensity calculated from monthly precipitation and the number of wet days. The land use pressure is based on the land cover simulations of the IMAGE model using index values specific for each crop or land cover type.

Apart from the uncertainty in climate projections, the actual land degradation strongly depends on the conservation measures taken to prevent soil erosion. The results of the land-degration model of IMAGE can therefore only be used to indentify regions where problems of water erosion may present and where they may be most severe, and how the land's sensitivity to water erosion may change in the future under scenarios of population growth, economic growth, technological development and climate change.

1 Introduction

Food security is of paramount importance in many countries of the world. With growing world population and economic growth the demand for food and feed will continue to increase in the coming decades. This rise in production can be achieved by intensification of existing agricultural land, and by opening new land for agricultural production.

Food security may be threatened by loss of soil productivity as a result of human-induced land degradation, which has affected about 15% of the global land surface (Oldeman *et al.,* 1990). Water and wind erosion can cause the loss of a considerable amount of topsoil (Follett and Stewart, 1985).

Even at moderate soil loss rates the associated losses of soil nutrients may be considerable. The translocated soil may contain 1.3-5 times as much organic matter as the soil remaining (Allison, 1973). As mineralization of soil organic matter is an important source of nitrogen and particularly phosphorous, soil organic matter is an important factor in determining the soil's fertility. In addition, soil organic matter plays and important role of stabilizing the soil's physical structure (Bouwman and Leemans, 1995).

Thus, important on-site effects of erosion may be a decline in qualities of soil related to agricultural productivity, while negative off-site effects such as over-blowing (wind erosion), or sedimentation of lakes and reservoirs (water erosion) may also occur.

Reversibility and time span determine the seriousness of degradation processes (Table 1.1). In addition, their spatial distribution on earth determines the extent of the most serious forms of land degradation. Water erosion is the most important cause of land degradation (Table 1.1), and its effects are irreversible. Wind erosion is important in drylands and areas with landforms conducive to high wind velocities. Chemical degradation, such as salinization, mineral weathering and nutrient loss, accounts for a small proportion of degraded lands, but over 40% of cropland degradation. Physical degradation (for example, compaction by animals, heavy machinery) accounts for only a small proportion of overall degraded area.

Changes in climate, the characteristics of land and soil at a specific location and changes in vegetation cover determine changes in the quality of soils and inherently influence the potential crop productivity with respect to agricultural use (Varallyay, 1990).

Land degradation and the loss of soil productivity in both the existing agricultural land and in future expansions may become very important for future sustainability and food security (Scher and Yadav, 1994). To address questions of food security in a changing world, the description of the role of land degradation is essential in the integrated assessment model IMAGE (Alcamo et al., 1998).

This report describes the approach followed for modelling the land's current and future sensitivity to land degradation in the IMAGE framework. The model description will be limited to the process of water erosion, the principal cause of land degradation.

Table 1.1. Land degradation processes, their time scale and reversibility and extent.

A. Degradation process	Time span (years)	Reversibility
Salinization (caused by desertification)	0.1 – 2	Yes
Acidification (drainage of marshy areas with cat-clays)	0.5 – 5	Yes
Decomposition of organic matter (by increased temperature)	5 – 20	Hardly
Accelerated erosion (water and wind erosion caused by decreased vegetation cover, increased precipitation)	10 – 50	Hardly
Accelerated mineral weathering (increased temperature/precipitation)	$10^2 – 10^4$	No
B. Erosion process	Affected area (% of global land area)	
Water erosion	8	
wind erosion	4	
Chemical degradation	2	
Physical degradation	1	
Total	15	

Source: Oldeman et al. (1990).

Recently, ISRIC published the results of a number of studies commissioned by RIVM on water erosion at different scales, ranging from the continental to national-scale:

- A global assessment of the vulnerability of land to water erosion at a scale of 1:5M, on a ½° x ½° grid, for instance using the WISE[1] database (Batjes, 1996a).
- A qualitative assessment of water erosion vulnerability at a scale of 1:5M, for a small section of the SOTER[1] database of Latin America (Batjes, 1996b).
- A mixed qualitative/quantitative assessment on the impact of water erosion on food productivity using the 1:1M SOTER[1] databases of Argentina, Uruguay and Kenya (Mantel and Van Engelen, 1997; 1999).

The above studies, in particular Batjes (1996a), formed the basis for the work described in this report. It is obvious that it is impossible to describe different water erosion processes, such as sheet, rill, gully and stream bank erosion, and estimate soil loss rates and effects on plant productivity, at the scale of the IMAGE calculations (0.5°). One of the questions that were addressed by Batjes (1996a) was how to describe the land's vulnerability to water erosion in a qualitative sense.

The purpose of the work described in this report is to develop an approach which allows for indicating where problems of water erosion may present and where they may be most severe, and how the land's sensitivity to water erosion may change in the future under scenarios of population growth, economic growth, technological development and climate change. In contrast to Batjes (1996a), we will not use the concept 'vulnerability' but use sensitivity instead. Vulnerability includes coping abilities, while sensitivity depicts a system possible response. A sensitive system does not need to be vulnerable, when it can adapt.

[1] At ISRIC two global soil and land databases are developed in cooperation with UNEP, ISSS and FAO: (i) WISE (World Inventory of Soil Emissions) contains the most important soil profile data (derived from over 4300 sites) related to the FAO 1:5M soil map of the world. (ii) SOTER (1:1M SOil and TERrain database) contains soil type descriptions related to the most important physiographic features at a regional scale level. SOTER permits geographic quantification and characterization of areas of concern (e.g. desertification, land degradation, soil pollution). SOTER is available for Latin America and parts of Africa and Asia; full world coverage will take another 10-20 years.

In the qualitative approach discussed in this report, a number of important concepts are used that may need explanation. These include susceptibility and sensitivity to water erosion, and the description of the protection against rainfall erosion as a function of land cover/use type as used in this report:

- The land's susceptibility to water erosion is based on the current soil and terrain erodibility and rainfall erosivity, ignoring the land use. Hence, it represents the sensitivity to water erosion of bare soil surfaces.
- Sensitivity to water erosion describes the chance for short-term occurrence of water erosion under current conditions of terrain erodibility, rainfall erosivity and land cover and use. The sensitivity taking into account the actual land use and cover, is low under natural vegetation, which provides maximum protection. Under agricultural systems the actual sensitivity depends on the type of crop.
- The description of land cover/use included in the sensitivity concept does not include descriptions of specific agronomic and mechanical soil conservation practices. The model developed, however, offers the possibility to modify the effect of soil conservation and other management practices to analyze the changes in sensitivity to water erosion.

In chapter 2 we will discuss the water erosion model as it was implemented in IMAGE 2 and the validation of the model results for the present situation. Chapter 3 describes some scenario calculations performed in the framework of the Fifth Environmental Outlook of RIVM.

2 Elaboration of a global water erosion sensitivity module

2.1. Introduction

The first version of a generalized global water erosion model presented by Batjes (1986a) is based on the Universal Soil Loss Equation (USLE) (Wischmeier and Smith, 1978). USLE is an approach for the assessment of the intensity of sheet and rill erosion on a field basis. It was developed for the eastern part of the USA to compute soil loss by rainfall from agricultural land, using regression equations based on local data for rainfall, soil and terrain characteristics, vegetation and management practices.

Application of the USLE at the global scale requires modification on the basis of the scale and the availability of data on climate, terrain characteristics and land management. First, instead of producing quantitative estimates of soil loss, at the global scale the assessment or erosion sensitivity should be qualitative. This requires simplification to make USLE suitable for the scale of calculations (0.5 by 0.5 degree), and adjustment of some of the parameters in the equation. This simplification was proposed by Batjes (1996a) who developed a generalized model for assessing qualitative water erosion hazard at a global resolution of 0.5º longitude x 0.5º latitude:

$$E = f(T, R, V) \tag{1}$$

with: E - erosion hazard
T - terrain erodibility index (considering slope and soil type)
R - rainfall erosivity index
V - land cover index

A detailed description of T, R and V as proposed by Batjes (1996a) is given in Appendix 1. The studies of Batjes (1996a;b) and Mantel and Van Engelen (1997; 1999) formed a starting point for a water erosion module for implementation in IMAGE. The general approach proposed by Batjes (1996a) and followed in this report is presented in Figure 2.1.

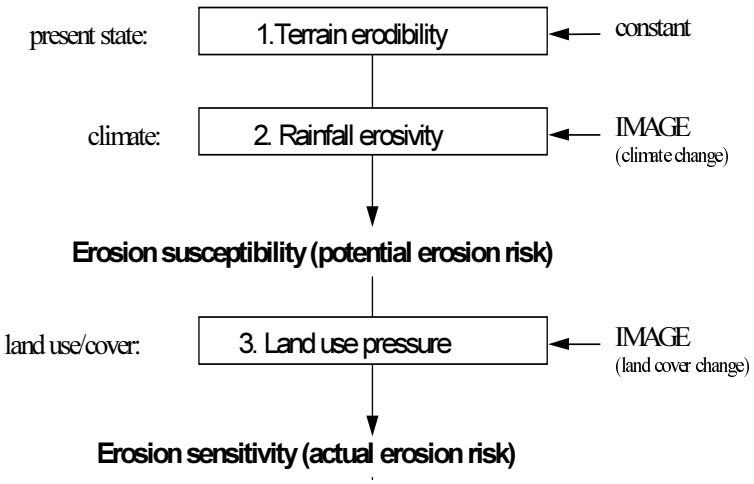

Figure 2.1. Scheme showing the calculation procedure of erosion sensitivity.

Some modifications of the approach of Batjes (1996a) were necessary for avoiding early classification as well as for enabling the dynamic application of scenario-based future changes in climate and land cover. The classification is not done for each component separately (soil texture, soil bulk density, soil depth, relief, rainfall erosivity and land use), but in the final rating of the susceptibility and sensitivity to water erosion.

The relief index based on the slope angle classification proposed by Batjes (1996a) was replaced by a landform characterization from a digital elevation model. For this reason, the rating of soil characteristics is referred to as soil erodibility. The combination of soil erodibility and the landform characterization yields the terrain erodibility.

The calculation of the rainfall erosivity is based on the annual rainfall distribution generated by IMAGE, instead of an indicator based on annual precipitation and zonal characteristics (Batjes, 1996a). The land use pressure is based on the land cover simulations of the IMAGE model.

The different components of the model implemented in IMAGE are discussed in more detail below.

2.2. Terrain erodibility (*T*)

The rating of soil characteristics is related to a rasterized version of the FAO Soil Map of the World (1991) on a 0.5°x0.5° grid. Each grid cell can include 1 to 8 different soil types and their characteristics are deduced from the WISE database. Consequently, the rating of terrain erodibility can be based on the dominant soil type, the most vulnerable soil type or the mean of soil properties.

The program code which is integrated in the IMAGE model leaves this option open to scenario considerations to avoid early classification. To avoid early classification, a continuous scale is used for soil characteristics, instead of the classes proposed by Batjes (1996a). For reasons of calculation efficiency the erodibility scale is reversed: the value 0 corresponds to least erodible, the value 1 to most erodible (which is different from the scale of Batjes (1996a) in Appendix 1).

The terrain erodibility is composed of indices for soil erodibility (*SE*) and the relief or landform (I_a). Soil erodibility in turn, is a combination of indices for soil texture, soil bulk density and soil depth.

2.2.1. Soil texture index (I_t)

Silty soils (silt is the particle size fraction between 2μm and 50μm) are distinguished as most erodible. Soils rich in clay (<2μm) are least erodible, while sandy soils (sand is the fraction >50μm) have intermediate erodibility. A function was defined to describe the soil texture effect per sé on the soil erodibility. Texture data for 0.5^o grid cells are taken from the WISE database. This function loosely follows the original relation of Wischmeier and Smith (1978):

$$I_t = -0.005 \times \mathrm{Cl}_s + 0.005 \times \mathrm{Si}_s + 0.5 \qquad (2)$$

with: I_t = texture index
Cl_s = clay content of soil type s (%)
Si_s = silt content of soil type s (%)

Table 2.1: Examples of the calculation of the soil texture index (I_t).

Soil type	Clay content (%)	Silt content (%)	I_t
gelic Regosols (silt loam)	25.0	63.5	0.69
ferric Podzols (sand)	3.0	9.0	0.53
pellic Vertisols (clay)	55.7	22.1	0.33
dystric Histosols (organic)	47.5	23.7	0.38
Lithosols (loam)	24.5	30.6	0.53

The results of equation (2) are given for example soil types in Table 2.1. In general, soils with a high silt content have a high soil texture index value, while soils rich in clay have a low texture index value.

2.2.2. Bulk density index (I_b)

The erodibility of the soil is further determined by the soil's structure. As descriptions of structure are difficult to obtain at the working scale of 0.5°, an approximation has to be used. The bulk density of the topsoil generally gives a fair representation of the porosity, and thus of soil structure (Batjes, 1996a). Soils with high bulk density have a low porosity, water does not easily infiltrate causing rainfall to easily run off easily from bare soil surfaces. Soils with low bulk density contain a relatively large amount of pores, water infiltrates more easily and run-off rates will be lower than on soils with high bulk density.

Following Batjes (1996a) soils with a bulk density larger than 1.55g cm^{-3} are considered most erodible; soils with a bulk density smaller than 1.15g cm^{-3} are least erodible (most often these are soils with a high organic matter content). Between these thresholds a simple linear relation is assumed (Table 2.2):

$$\mathrm{bd}_s < 1.15 \rightarrow I_b = 0; \quad (3)$$

$$1.15 < \mathrm{bd}_s < 1.55 \rightarrow I_b = 2.5 \times \mathrm{bd}_s - 2.875 \quad (4)$$

$$\mathrm{bd}_s > 1.55 \rightarrow I_b = 1 \quad (5)$$

with: I_b = bulk density index
bd_s = bulk density ($g.cm^{-3}$)

2.2.3. Soil depth index (I_d)

Shallow soils on rock material have a low soil water storage capacity. Therefore, shallow soils are easily water-saturated after rainfall. On bare soil surfaces superficial run-off may occur under saturated conditions, and in extreme cases mud flows may cause massive soil translocation, depending on the properties of the soil and the underlying rock.

Table 2.2. Examples of the calculation of the bulk density index (I_b)

Soil type	Bulk density[1]	I_b
gelic Regosols (silt loam)	1.51	0.90
ferric Podzols (sand)	1.32	0.43
pellic Vertisols (clay)	1.59	1.0
dystric Histosols (organic)	0.31	0.0
Lithosols (loam)	1.42	0.68

[1] Bulk density in g cm^{-3}

Table 2.3. Soil depth classes and corresponding values of the soil depth index (I_d).

Soil depth (cm)	I_d
0-25	1.0
25-50	0.9
50-100	0.6
100-150	0.25
<150	0.0

Soil depth classes are given for each soil type in the WISE database. As in Batjes (1996a) these classes are converted to an index scale to enable quantitative combination with the other two soil indices (Tables 2.3 and 2.4).

Table 2.4. Examples of the soil depth index for different soil (I_d).

Soil type	Soil depth (cm)	I_d
gelic Regosols (silt loam)	50-100	0.60
ferric Podzols (sand)	>150	0.0
pellic Vertisols (clay)	>150	0.0
dystric Histosols (organic)	>150	0.0
Lithosols (loam)	0-25	1.0

2.2.4. Soil erodibility (*SE*)

The soil erodibility (*SE*) is derived from three soil indices for texture, bulk density and soil depth (I_t, I_b and I_d) by taking the average of the 2 maximum values. Although this approach is rather arbitrarily chosen, it will result in a qualitative expression of the relative differences between soils, as shown in Table 2.5.

*Table 2.5. Examples of the determination of the soil erodibility (*SE*).*

Soil type	I_t	I_b	I_d	SE
gelic Regosols (silt loam)	0.69	0.90	0.60	0.80
ferric Podzols (sand)	0.53	0.43	0.0	0.48
pellic Vertisols (clay)	0.33	1.0	0.0	0.67
dystric Histosols (organic)	0.38	0.0	0.0	0.19
Lithosols (loam)	0.53	0.68	1.0	0.61

2.2.5. Relief index (I_a)

The FAO Soil Map of the World (1991) gives slope angle classes for each soil polygon, which can stretch over multiple 0.5°x0.5° grid cells. The slope classes defined by FAO cover a wide range of slope angles, i.e. 0-8%, 8-30% and >30%. Although combinations of these classes occur on the soil map, the classes were considered to be have insufficient detail even for a qualitative assessment of erosion sensitivity.

Therefore, in this model an expression of slopes is derived from a global digital elevation model. Landforms were characterized on the basis of the 10 minute grid FNOC elevation data

Table 2.6. Examples of the calculation of the relief index (I_a).

Soil type	Slope angle class[1]	Relief character[2]	I_a
gelic Regosols (silt loam)	b	>300	1.0
ferric Podzols (sand)	b	210	0.70
pellic Vertisols (clay)	a	100	0.33
dystric Histosols (organic)	a	30	0.10
Lithosols (loam)	c	>300	1.0

[1] Slope angle class from FAO soil map of the world: a: <8%; b: 8-30%; c: >30%: these values are unique per soil polygon.
[2] Difference between maximum and minimum altitude within grid cell in m (derived from digital elevation model). These values are unique per grid cell and not linked to soil type.

set (FNOC, 1985). Each grid cell in this data set contains data on mean elevation, and the minimum and maximum altitude. The difference between minimum and maximum altitude is transferred to the relief index (I_a) that specifies the general landform (flat, undulating, mountainous, etc.). The use of a unique relief index per grid cell introduces variability among grid cells that cover the same soil polygon.

Comparison with the GLASOD database indicated that areas with a severe erosion status mostly cover cells with an elevation difference of more than 300m. These cells are therefore indicated as most susceptible to erosion, whereas cells with a smaller elevation difference follow a simple linear relation:

$$(\mathrm{alt}_{\max} - \mathrm{alt}_{\min}) < 300\,\mathrm{m} \rightarrow I_a = \frac{1}{300} \times (\mathrm{alt}_{\max} - \mathrm{alt}_{\min}) \quad (6)$$

$$(\mathrm{alt}_{\max} - \mathrm{alt}_{\min}) > 300m \rightarrow I_a = 1 \quad (7)$$

with: I_a = indicator for landform
$\mathrm{alt}_{\max}$ = maximum altitude (m)
$\mathrm{alt}_{\min}$ = minimum altitude (m)

This method results in a unique relief index for each grid cell. It is therefore not representative for specific soil polygons or soil types as in FAO (1991).

2.2.6. Terrain erodibility (*T*)

The terrain erodibility expresses the combined susceptibility of soil and relief. Hence, the land cover and use are not included, hence it expresses the relative susceptibility of bare soil with a given slope.

Terrain erodibility (T) is defined as the average of soil erodibility and the relief indices. The weight assigned to the combined soil indices I_t, I_b and I_d equals that of the relief index (I_a). In the approach proposed by Batjes (1996a) equal weights were used for the individual soil indices and the relief. In our modified approach the terrain erodibility for a highly susceptible soil in a flat terrain is lower than according to Batjes (1996a). The results for a selection of soil types for the terrain erodibility index are presented in Table 2.7.

The resulting terrain erodibility index is shown in Figure 2.2. The areas with high index values represent a strong geographic relief, such as the hilly and mountainous part of North and South America, the Alps in Europe, the Ural in Eurasia, the massive in the northern part

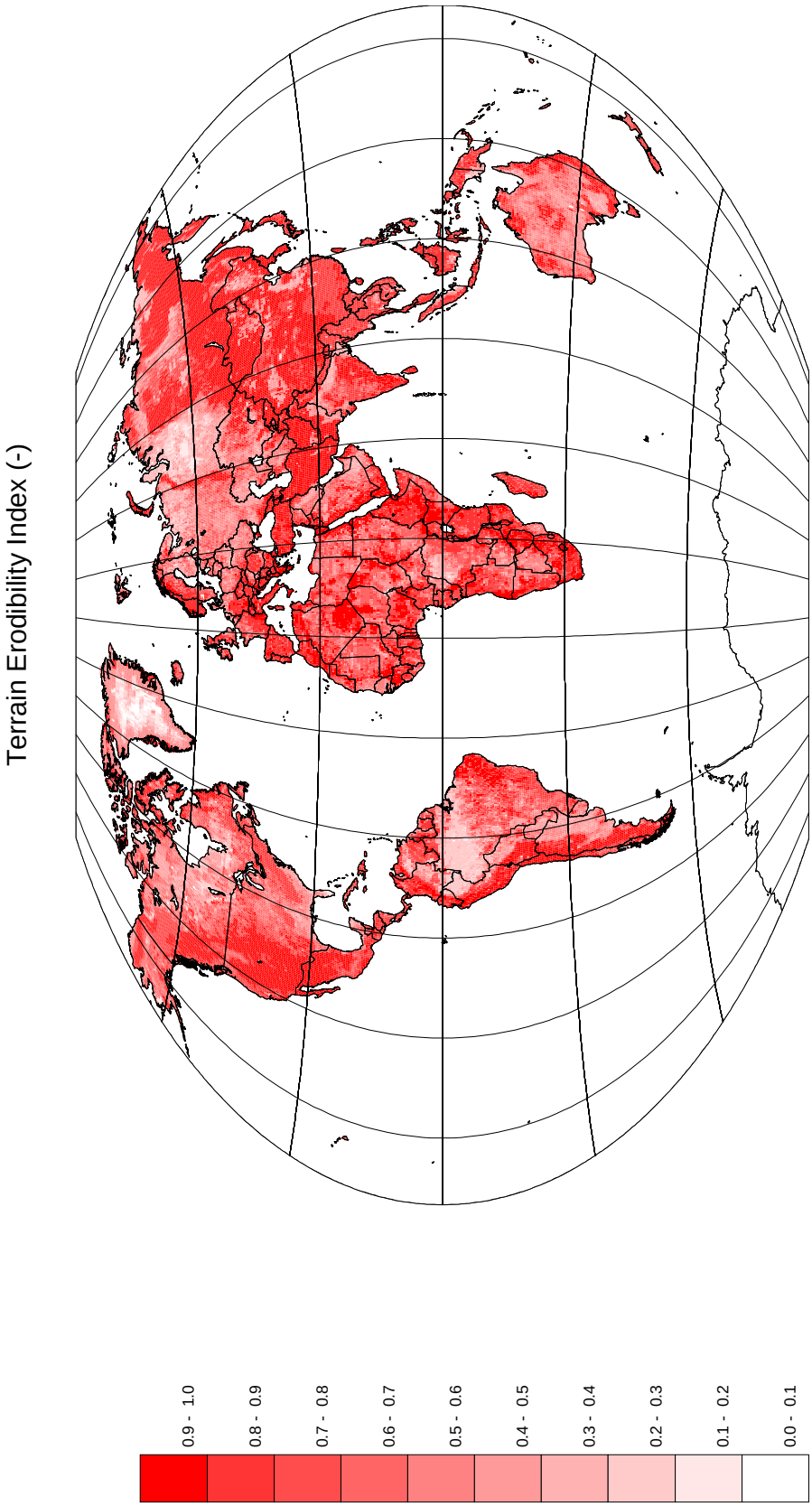

Figure 2.2. Terrain erodibility index for 1995 (IMAGE team, 2001).

of Iraq, Iran, and Afghanistan, the mountainous parts of North and East Africa, and of Asia (Himalayas, north-eastern part of the former USSR).

The terrain erodibility index is assumed not to be subject to changes in the future. The values of the parameters that are used to calculate the terrain erodibility for 1990 are therefore used for all future simulations.

*Table 2.7. Examples of the calculation of the terrain erodibility index (*T*).*

Soil type	*SE*	I_a	*T*
gelic Regosols (silt loam)	0.80	1.0	0.90
ferric Podzols (sand)	0.48	0.70	0.59
pellic Vertisols (clay)	0.67	0.33	0.50
dystric Histosols (organic)	0.19	0.10	0.15
Lithosols (loam)	0.61	1.0	0.81

2.3. Rainfall erosivity (*R*)

Batjes (1996a) used data available from the Agro-Ecological Zones map (De Pauw et al., 1996) and Bouwman (1989) to derive the present rainfall erosivity index. Bouwman (1989) used a straightforward relation between annual precipitation and rainfall erosivity. In contrast, Hoekstra (1995) used monthly precipitation to describe the rainfall distribution during the year. However, this method does not distinguish between differences in rainfall intensity.

As soil loss generally occurs during showers of high intensity, the month with maximum rainfall intensity is considered to be indicative for rainfall erosivity. For the IMAGE-erosion modelling an indication of rainfall intensity was inferred from the monthly precipitation values and the number of wet days. The monthly mean rainfall intensity (mm/day) is calculated as monthly precipitation divided by number of wet days in each month from the climate data of Leemans and Cramer (1991).

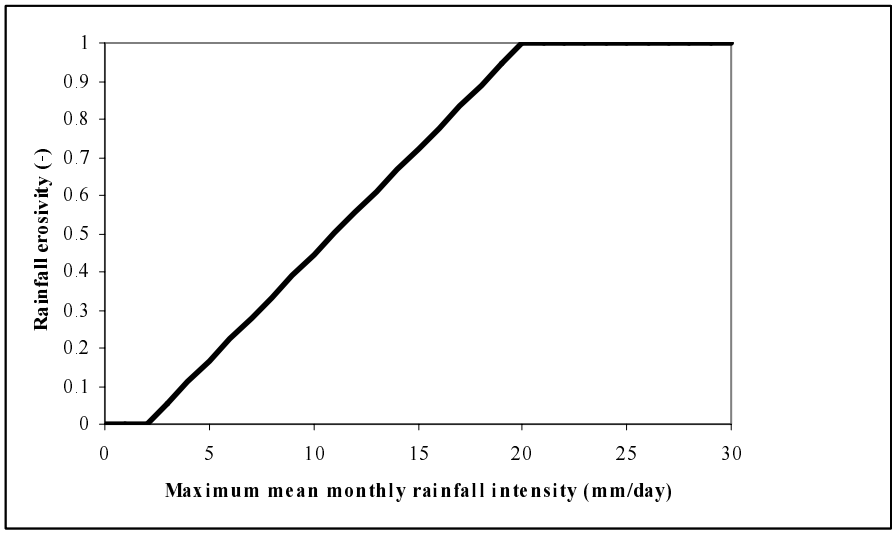

Figure 2.3. Rainfall erosivity inex as a function of the maximum mean monthly rainfall intensity.

For each grid cell the maximum mean monthly rainfall intensity is converted into an index on the basis of the following assumptions. Maximum mean monthly rainfall intensities of 0-2 mm/day are assigned an index value of 0, while those exceeding 20mm/day are assigned an index value of 1.0. Between these two extremes a linear relation is assumed (Figure 2.3).

It should be noted that the concept of maximum mean monthly rainfall intensity used here is different from the intensity of individual rain showers. However, mean intensities of 20 mm/day corresponding to an index value of 1.0 will likely be accompanied by individual rain shower intensities that largely exceed this mean value.

The resulting map of rainfall erosivity for 1995 clearly indicates the areas that are actually prone to high rainfall erosivity (e.g. the regions with a Mediterranean type of climate) (Figure 2.4). The results of our approach shows a rather high rainfall erosivity index in the regions surrounding the equator, India and southeastern part of China, and in some parts of Central Europe.

In the IMAGE erosion modelling rainfall erosivity is made dynamic by its re-scaling with the generated changes in precipitation based on different scenarios for future years. The number of wet days is assumed to be constant in time, as the IMAGE model does not generate projections for this aspect.

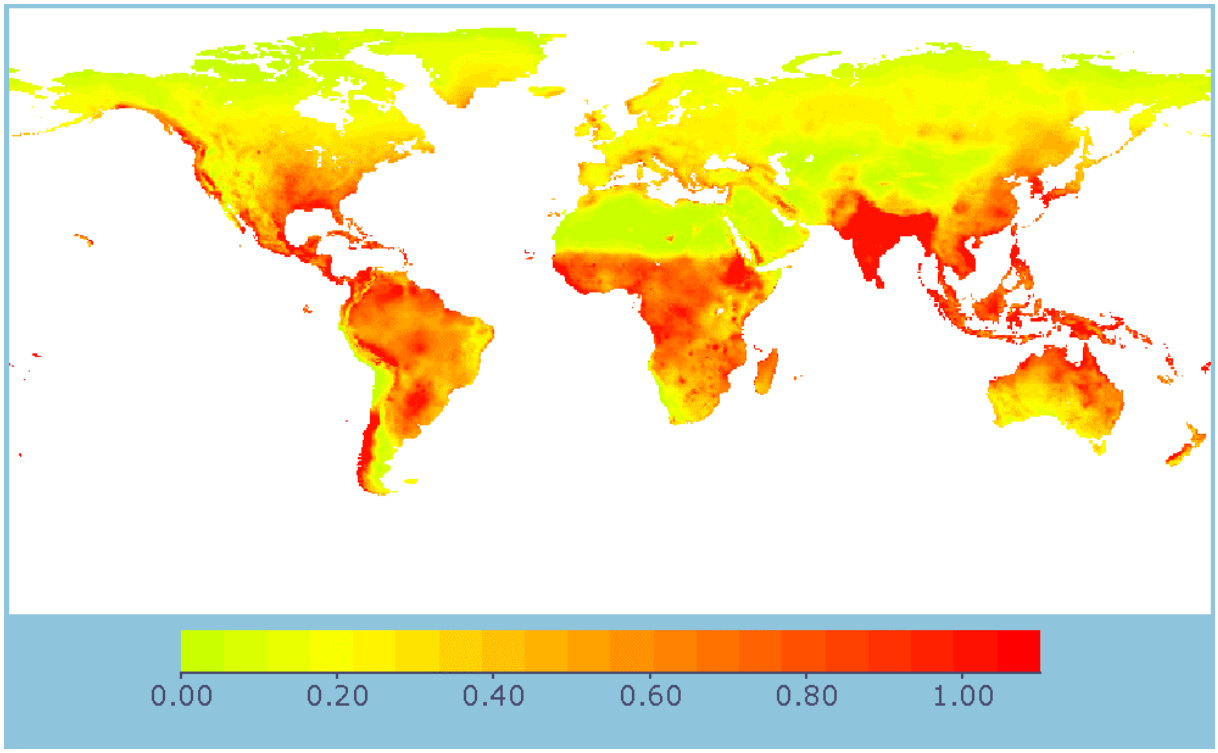

Figure 2.4. Rainfall erosivity index for 1970 (see also Figure 3.1)(IMAGE team, 2001)

2.4. Susceptibility to erosion (E_p)

The combination of rainfall erosivity (*R*) with terrain erodibility (*T*) finally yields an estimate of the potential susceptibility of the land based on factors of climate and terrain. This potential susceptibility is referred to as erosion susceptibility (*Ep*):

$$E_p = \frac{R+T}{2} \in [0,1] \tag{8}$$

An alternative to equation (8) is to use the minimum of both indices to indicate erosion susceptibility, because if either of the two indices is very low, then erosion will not likely occur. However, the purpose of this modelling approach is to produce a qualitative assessment of relative differences in current erosion risk, and future changes as a consequence of land cover/use and climate change. Therefore, it was considered justified to use the average of rainfall erosivity and soil erodibility.

2.5. Land cover/use index (*LUI*)

Land cover and use pressure are important determinants of the actual sensitivity to water erosion. As the IMAGE model produces land cover maps containing the geographic distribution of different land cover types, this information forms the basis for estimating current and future land cover/use index.

Natural vegetation such as forests provide a high degree of protection against rainfall erosion, while agriculture generally leads to the higher sensitivity of the land surface to the destructive action of intensive rainfall. Table 2.8 presents land cover/use indices (*LUI*) for various land cover types. Most values were derived from Wood and Dent (1983).

*Table 2.8. Land cover/use index for different land cover types (*V*).*

Land cover type	Crop type	Land use intensity index (*LUI*)
Agriculture	grass[1]	0.40
	temperate cereals	0.65
	rice[1,2]	0.50
	maize	0.95
	tropical cereals	0.65
	pulses	0.65
	roots and tubers	0.85
	oil crops	0.80
	sugar cane	0.55
	woody biofuels[1]	0.40
	non-woody biofuels[1]	0.55
Extensive grassland[1]		0.40
Re-growth forest, scrubland, tropical woodland[1]		0.15
Other land cover types		0

Based on Wood and Dent (1983) unless indicated otherwise. High index values indicate high sensitivity to rainfall erosion.

[1] Different from Wood and Dent (1983) who proposed values of 0.01 for grass and wetland rice. These values were adjusted after visual comparison with GLASOD.

[2] Estimated value for wetland rice; upland rice can have values up to 0.65.

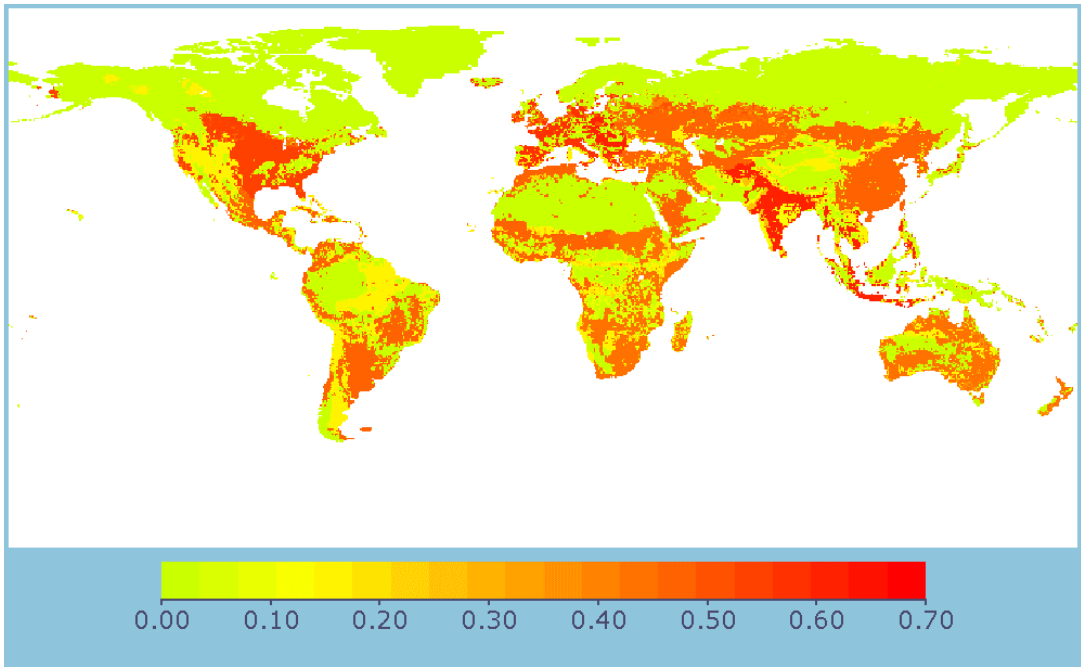

Figure 2.5. Land use/cover index for 1995 (IMAGE team, 2001).

For the non-agricultural land cover types the value for V is derived directly from Table 2.8. A grid cell (partly) covered by agricultural crops is assigned a composite value for V, which is based on the distribution of agricultural crops within the specific world region (see Alcamo et al., 1998) to which the grid cell belongs:

$$V_r = \sum_{i=1}^{c} f_{i,r} \times LUI_i \tag{9}$$

with: V_r = land cover/use index in region r
r = region number
$f_{i,r}$ = fraction of crop i in region r
c = number of crops
LUI_i = Land cover/use index for crop i (see Table 2.8).

This method allows for estimating future changes in the land's sensitivity to water erosion on the basis of future developments in land cover/use generated by the IMAGE model. The distribution for 1995 is presented in Figure 2.5. The contribution of soil and crop management and soil conservation practices are not included in the land cover/use index. However, the model described here allows for adapting the land cover/use index to assess future consequences for water erosion sensitivity.

2.6. Erosion sensitivity

The sensitivity to water erosion (Ea) is derived by combining the land's susceptibility to erosion (Ep) with the land cover/use index (V) as follows:

$$E_a = V \times E_p \tag{10}$$

Combination by multiplying of the indices V and E_p with opposite scales a compensation of effects is achieved. For example, for low values of V (high degree of protection provided by

Table 2.9. Classification of water erosion sensitivity index.

E_a index	E_a classification
< 0.15	no/low erosion risk
0.15 - 0.30	moderate
0.30 - 0.45	high
> 0.45	very high erosion risk

the land's cover), and high land susceptibility (high value of E_p), the sensitivity to water erosion will still be low. Contrary, when the protection provided by the land's cover is low e.g., under agriculture), the sensitivity will be low if the land's susceptibility is low (for example on non-sloping land).

Section 2.7 addresses the validation of the results based on equation (10), and the classification of the index E_a.

2.7. Validation of the global results

Visual comparison of the results for the sensitivity to erosion (E_a) discussed in section 2.6 with data on the status of land degradation caused by water erosion from Oldeman et al (1990) shows a good agreement, even though the concept of erosion risk and erosion status are different.

We have developed a classification of the index for the erosion sensitivity index for comparison with the GLASOD degradation status caused by water erosion of Oldeman et al. (1990). In developing this classification we considered a low sensitivity and high degree of land degradation due to water erosion to be inconsistent. Preferably, each grid cell should have a sensitivity to erosion that is equal to or higher than the actual erosion status.

By trial and error we have attempted to achieve maximum correspondence. Using the classification of sensitivity to erosion as given in Table 2.9, approximately 85% of the grid cells have a calculated erosion risk which is equal to or higher than the GLASOD water erosion status.

3 Results

We have performed calculations with the IMAGE 2.1.2 model on the basis of three scenarios from the IPCC Special Report on Emission Scenarios (SRES) (IPCC, 2000) for the Fifth Environmental Forecast (MV5). The water erosion model used was a stand-alone version. The model has also been incorporated in the Terrestrial Environment System (TES) of IMAGE 2.2.

The terrain erodibility is assumed to be constant, since in the IMAGE model soil and terrain characteristics do not change. This is not the case for the rainfall erosivity and the land use index. As outlined in Chapter 2 the dynamics in rainfall erosivity is introduced through a process of re-scaling the precipitation as derived from IMAGE using the 1990 database for the monthly number of wet days. Increasing rainfall erosivity according to the IMAGE calculations based on the HCM2 climate model results is expected to occur especially in Eurasia, southern parts Australia, North America (except the area west of the plains) and Central America (Figure 3.1 and 3.2). In these areas the increase can be significant (from a very low or low index value to a medium index values by 2050).

The erosion sensitivity calculated according to equation (10) combines the terrain erodibility, rainfall erosivity and the land use index (Figure 3.3). According to the scenario under consideration the sensitivity is expected to increase considerable in several world regions (Figure 5). Figure 3.3 shows the situation in 1995. The results shown in Figure 3.4 (based on IMAGE 2.1.2) indicate that in regions such as Africa, Latin America and Asia, where the erosion sensitivity is already high, the increase in erosion sensitivity is stronger than in high-income countries. In these regions, such as North America and Europe, where land use changes are less important than in low-income countries, the erosion sensitivity increases much less as a result of changing rainfall erosivity (climate).

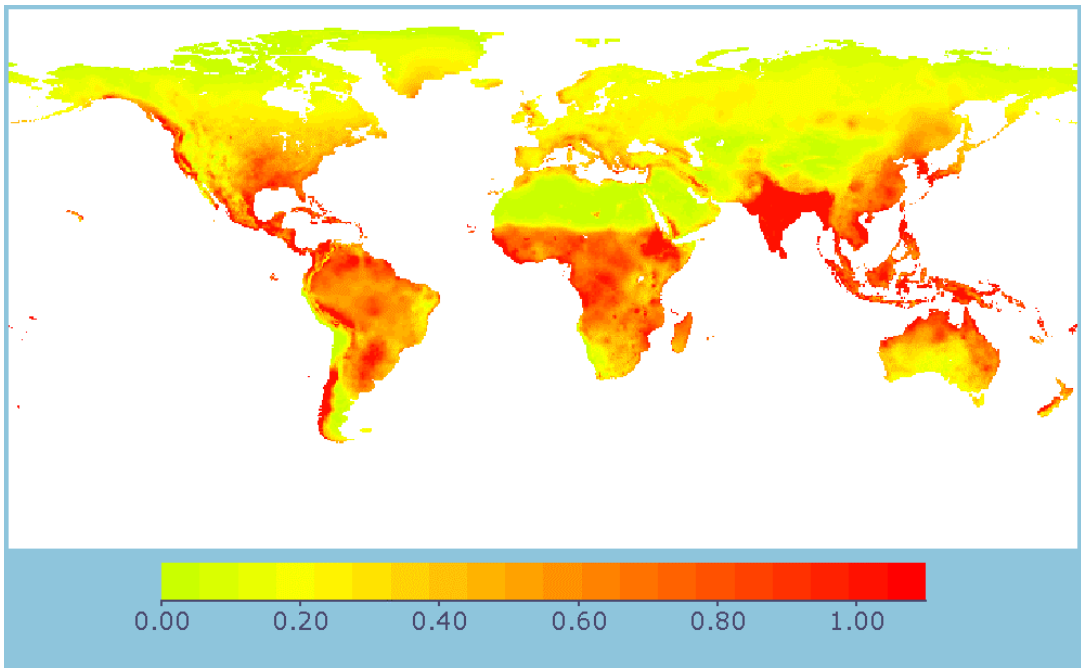

Figure 3.1. Rainfall erosivity index for 1995 (IMAGE team, 2001).

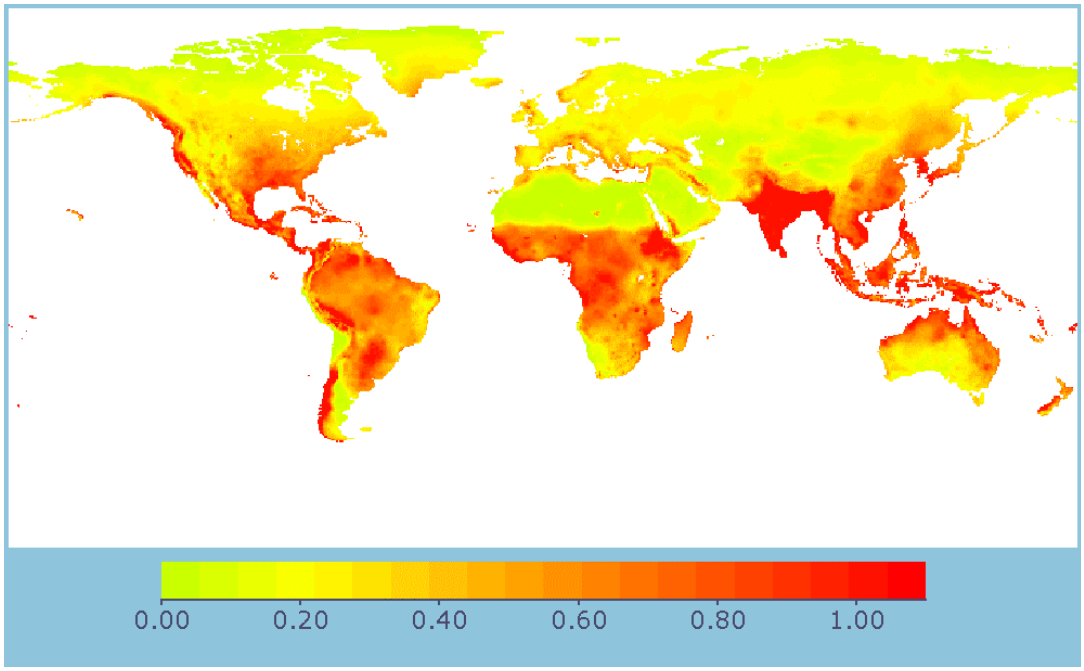

Figure 3.2. Rainfall erosivity index for 2050 according to theHADCM2 climate model (IMAGE team, 2001).

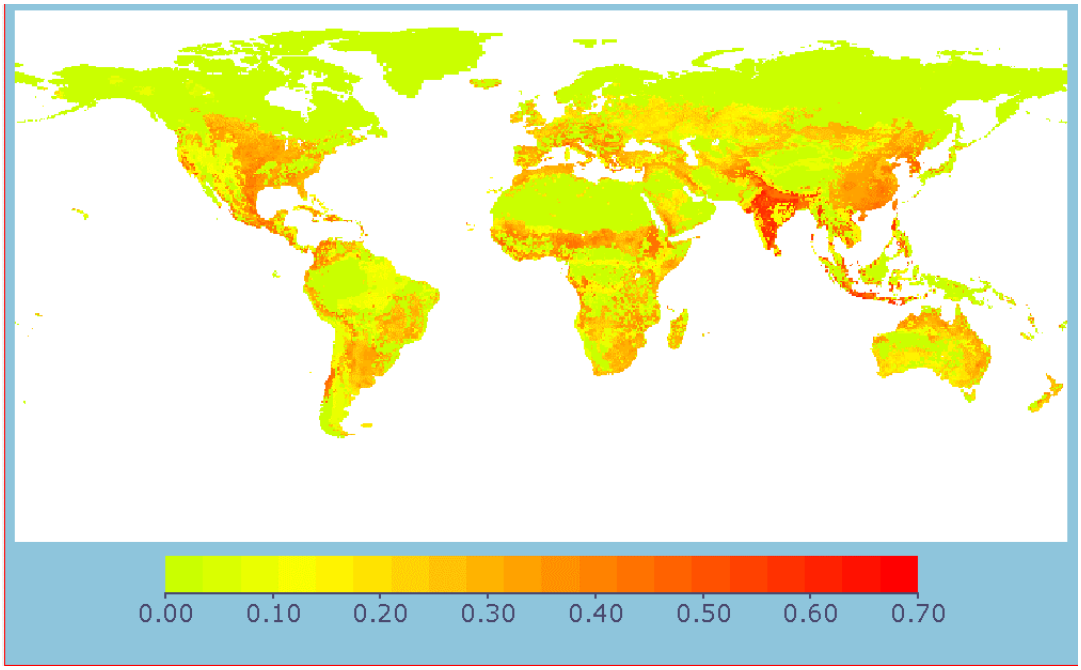

Figure 3.3. Rainfall erosion sensitivity index for 1995 (IMAGE team, 2001).

One of the sources of uncertainty in the estimation of future risk of land degradation is climate change. Differences in estimates of the area in the high and very high risk class for the erosion sensitivity calculated on the basis of different climate models are presented in Table 3.1. We used the results from different climate models (CGCM, CSIR, HCM3, PMI4 and HCM2) for regional climate changes resulting from the same scenario for emissions of greenhouse gases and land use. The largest differences between climate models for the A1 scenario in the erosion sensitivity is found in the Middle East and East Asia. In the USA, Africa and South Asia the differences between climate models are much less pronounced.

Table 3.1. Areas of land in the high and very-high classes of the erosion vlunerability index calculated for three IPCC-SRES scenarios and different climate models.

	A1					B1	B2
	% of land area						
	CGCM	CSIR	HCM3	MPI4	HCM2	HCM2	HCM2
Canada	1	1	1	1	1	1	1
USA	29	16	21	25	21	18	16
Latin America	20	17	16	20	17	14	15
Africa	28	25	28	32	26	24	36
OECD Europe	19	16	16	19	15	12	11
Eastern Europe	19	15	14	21	13	11	8
CIS	2	1	1	2	1	0	0
Middle East	33	8	8	32	12	12	12
India + S. Asia	83	74	78	75	74	54	74
China + C.P. Asia	32	26	30	36	31	33	39
East Asia	26	25	26	28	26	25	38
Oceania	5	4	5	9	4	3	4
Japan	39	35	36	38	34	30	30

The CSIR climate model results consistently in the lowest erosion risk, while the CGCM consistently gives the highest risk. The MPI4 climate model yields a high risk in all regions. The differences for one single climate model and different scenarios (A1, B1 and B2) is negligible in some regions (such as Middle East) and very important in others (South Asia).

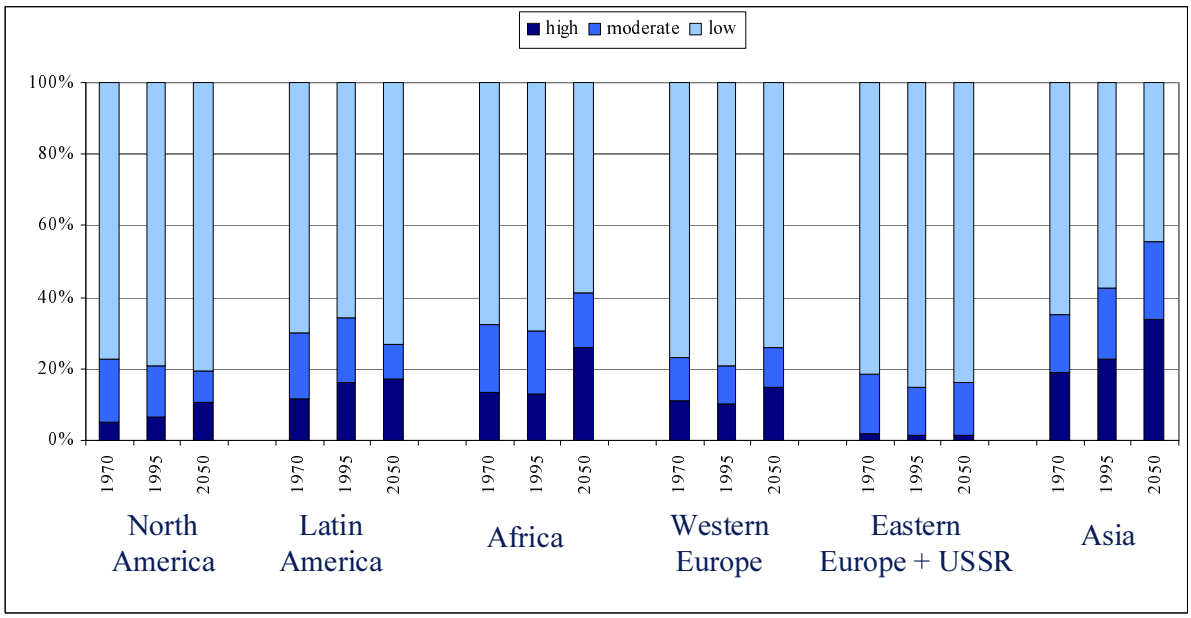

Figure 3.4. Risk of land degradation according to the IPCC-SRES A1 scenario expressed as the areas for three classes of the rainfall erosion sensitivity for different world regions (RIVM, 2000).

4 Conclusions

This report describes a model to describe the land's sensitivity to water erosion in a qualitative sense. For this purpose a modified version of the Universal Soil Loss Equation (USLE) was used. Application of the USLE at a global scale requires modification on the basis of the scale and the availability of data on climate, terrain characteristics and land management. The model developed is formulated as follows:

$$E = f(T, R, V) \tag{11}$$

with: E - erosion hazard
T - terrain erodibility index (considering slope and soil type)
R - rainfall erosivity index
V - land use/cover index

The terrain erodibility index is composed of the soil erodibility index and relief index. The soil erodibility index is based on soil texture and soil depth. The relief index is a landform characterization derived from a digital elevation model (based on differences in elevation within grid cells). The calculation of the rainfall erosivity is based on the maximum mean monthly rainfall intensity calculated from monthly precipitation and the number of wet days. The land use pressure is based on the land cover simulations of the IMAGE model using index values specific for each crop or land cover type.

Apart from the uncertainty in climate projections, the actual land degradation strongly depends on the conservation measures taken to prevent soil erosion. Furthermore, it is impossible to estimate soil loss rates and effects on plant productivity for different water erosion processes, such as sheet, rill, gully and stream bank erosion, at the scale of the IMAGE calculations (0.5^{o}). Finally, a major problem is that it is impossible to translate soil loss rates into effects on soil productivity as a result of loss of physical stability of chemical fertility.

The model developed therefore describes the land's sensitivity to water erosion in a qualitative sense. The results can be used to identify regions where problems of water erosion may present and where they may be most severe, and how the land's sensitivity to water erosion may change in the future under scenarios of population growth, economic growth, technological development and climate change. The model developed also offers the possibility to modify the effect of soil conservation and other management practices to analyze the changes in sensitivity to water erosion.

It is clear that some components of the land degradation model have weaknesses. At the 0.5^{o} by 0.5^{o} resolution of the calculations, which can be regarded as the scale of landscapes, the heterogeneity of soil and terrain conditions cannot be represented. The soil properties that determine the erodibility are given for 8 soil types per grid cell derived from the WISE database (Batjes, 1996a). The susceptibility to erosion is finally calculated as a weighted mean for the grid cell. This gives a generalized representation of the grid-cell, ignoring variability within the cell that may be important for land degradation.

A second problem is related to the relief or landform. This is represented in the model by the maximum difference in altitude for 10 minute grids within each 0.5^{o} by 0.5^{o} grid cell. This

means that part of the grid cell may be flat or undulating terrain, while the maximum altitude difference may still be >300 m, above which the relief index has the maximum value of 1.0. This approach could be improved by a true description of landforms in terms of slopes and slope length. Such a map could be produced from, for example, remote sensing data.

Further improvement of the model can be achieved by using coupled soil and plant production models to describe the effects of land use on chemical and physical properties of the soil. The major soil characteristic in this respect is soil organic matter. Such a model approach involves the description of the soil C and N cycle including inputs and decomposition of soil organic matter in dependence of land use, terrain characteristics and climate. Plant production models simulate the effect of soil fertility on the production of natural and agricultural ecosystems, and the production of above- and below ground litter, which forms the input of soil organic matter into the soil. Such an approach would also enable to describe effects of changing atmospheric CO_2 concentration, climate and atmospheric N deposition on net primary production, soil processes and soil degradation in an integrated model.

References

Alcamo, J., E. Kreileman and R. Leemans, eds. (1998) Global change scenarios of the 21st centure. Elsevier Science Publishers, Amsterdam.

Allison (1973) Soil organic matter and its role in crop production. Developments in Soil Science Vol. 3, Elsevier, Amsterdam, 637 pp.

Batjes, N.H. (1996a) Global assessment of land vulnerability to water erosion on a ½º by ½º grid. Land Degradation and Development 7, no. 4, p353-365.

Batjes, N.H. (1996b) A qualitative assessment of water erosion risk using the 1:5M SOTER database for northern Argentina, south-east Brazil and Uruguay. Wageningen: ISRIC, Working Paper 96/04.

Bouwman, A.F. (1989) Land evaluation for rainfed farming using global terrain information on a 1º longitude by 1º latitude grid. Working Paper and Preprint 89/01, ISRIC, Wageningen.

Bouwman, A.F. and R. Leemans (1985) The role of forest soils in the global carbon cycle. In: W.M. McFee and J.M. Kelly (Eds.) Carbon forms and functions in forest soils. pp. 503-525, Soil Science Society of America, Madison.

FAO (1991) The Digitized Soil Map of the World. Notes: Volume Africa. World Soil Resources Report 67/1 (release 1.0), FAO, Rome.

FNOC (1985) 10 minute Global Elevation, Terrain and Surface Characteristics, NOAA National Geophysical Data Center, Monterey (CA).

Follett, R.F. and B.A. Stewart (Eds.) (1985) Soil erosion and crop productivity. American Society of Agronomy, Crop Science Society of America, Soil Science Society of America, Madison, 533 pp.

Hoekstra, A.Y. (1995) AQUA - a framework for integrated water policy analysis. Bilthoven: RIVM report 461502006, Global Dynamics and Sustainable Development Programme Report Series no. 6.

Hudson, N. (1981) Soil conservation. Batsford Academic and Educational Ltd., London, 324 pp.

IMAGE team (2001) The IMAGE 2.2 implementation of the SRES scenarios. A comprehensive analysis of emissions, climate change and impacts in the 21st century. RIVM-publication 481508016, National Institute for Public Health and the Environment, Bilthoven, the Netherlands.

IPCC (2000) Special report on emission scenarios. A special report of Working Group III of the Intergovernmental Panel on Climate Change, Cambridge University press, 5999 pp.

Leemans, R. and W.P. Cramer (1991) The IIASA database for mean monthly values of temperature, precipitation, and cloudiness on a global terrestrial grid. RR-91-18, International Institute for Applied Systems Analysis, Laxenburg.

Mantel, S. and V.W.P. van Engelen (1997) The impact of land degradation on food productivity - case studies of Uruguay, Argentina and Kenya. Wageningen: ISRIC, Working Paper 97/01.

Mantel, S. and V.W.P. Van Engelen (1999) Assessment of the impact of water erosion on productivity of maize in kenya: an integrated modelling approach. Land degradation and Development 10:577-592.

Matthews, E. (1983) Global vegetation and land use: new high-resolution data bases for climate studies. Journal of Climate and Applied Meteorology 22:474-487.

Morgan, R.P.C. (1986) Soil erosion and conservation. Longman, Harlow, Essex, 298 pp.

Oldeman, L.R., R.T.A. Hakkeling and W.G. Sombroek (1990). World map of the status of human-induced soil degradation - an explanatory note (GLASOD). Wageningen: ISRIC, Nairobi: UNEP.

Pauw, E. de, F.O. Nachtergaele and J. Antoine (1996) A provisional world climate resource inventory based on the length-of-growing period concept. In Batjes, N.H., J.H. Kauffman and O. Spaargaren (eds.): Proceedings NASREC workshop, pp. 30-43, ISRIC, Wageningen.

RIVM (2000) Nationale milieuverkenning 2000-2030. National Institute for Public health and the Environment. Samson bv, Alphen aan den Rijn, 271 pp.

Scher, S.J. and S. Yadav (1994) Land degradation in the developing world: implications for food, agriculture and the environment to 2020. International Food Policy Research Institute: Food, Agriculture and the Environment Working Paper 14.

Varallyay, G.Y. (1990) Influence of climatic change on soil moisture regime, texture, structure and erosion. In Scharpenseel, H.W., M. Schomaker and A. Ayoud (eds.): Soils on a warmer earth - effects of expected climate change on soil processes, with emphasis on the tropics and sub-tropics, Developments in Soil Science 20, Elsevier, Amsterdam, pp. 39-49.

Wischmeier, W.H. and M.D. Smith (1978) Predicting Rainfall Erosion Losses - a Guide to Conservation Planning. Agricultural Handbook no. 537, US Dept of Agriculture, Washington DC.

Wood, S. R., and Dent, F. J. (1983) “LECS - A land evaluation computer system methodology”, Ministry of Agriculture Government of Indonesia, United Nations Food and Agriculture Organization, Bogor, Indonesia.

Appendix. Description of the ISRIC method for erosion sensitivity assessment

General

The Universal Soil Loss Equation (USLE) is an approach for the assessment of the intensity of sheet and rill erosion on a field basis (Wischmeier and Smith, 1978). The USLE was developed for the eastern part of the USA to compute soil loss by rainfall from agricultural land at field scale. The predicted soil loss (*A*), according to the USLE, is:

$$A = R \times K \times LS \times P \times C \quad \text{(A1)}$$

with: *R* - rainfall erosivity index
K - soil erodibility factor (a function of soil texture, structure, organic matter content and permeability)
LS - factor for slope angle and length (topography)
P - factor for management practices (including cultivation and soil conservation)
C - factor for vegetation density and structure

Application of the USLE in other climates and at a different (in this case global) scale requires adjustment of some parameters in the equation and a number of simplifications, dictated by the availability of data, their reliability and accuracy, as well as the required resolution. This also implies that instead of actual water erosion severity the model should be aimed at supplying an estimate of water erosion risk.

Batjes (1996a) proposed such a generalized model for assessing water erosion risk (*E*) at a global resolution of ½º longitude x ½º latitude:

$$E = f(T, R, V) \quad \text{(A2)}$$

with: *T* - terrain erodibility factor (considering slope and soil type)
R - rainfall erosivity index
V - factor for land cover

The characteristics of soil and terrain describe its *passive* sensitivity to water erosion. In the process of water erosion both rainfall erosivity and land use pressure play the role of *actors*. If both actors are sufficiently present, then the passive subject will be eroded to an extent indicated by its erodibility. A loamy soil (little coherence) on a steep slope will be eroded more easily than a clayey soil in a flat landscape. Therefore, the erodibility of the former soil will be higher than the latter soil. However, even a soil with a high erodibility is not necessarily prone to erosion. If the two actors of water erosion are absent, the soil will preserve its current condition. On the other hand, a soil with low erodibility can still be eroded severely, if rainfall erosivity and land use pressure are extremely strong. Consequently, erodibility should be seen as an indicator of the *relative* sensitivity of a soil to water erosion.

Terrain erodibility (*T*)

The physical characteristics of a soil and its position in a landscape reflect an intrinsic susceptibility to erosion by rainfall, also referred to as the terrain erodibility (*T*). The physical characteristics can be summarized by the stability of soil structure and the ability of the soil to absorb rainfall vs. superficial runoff, which can trigger erosion. In the assessment of terrain erodibility three soil characteristics (texture, bulk density and soil depth) and one terrain characteristic (an average regional slope angle per soil type) are considered.

For each soil unit from the FAO Soil Map of the World data from representative soil profile descriptions are available in ISRIC's WISE database. From this database, which consists of over 4,000 profile descriptions, the average characterization of soil texture, bulk density and soil depth can be deduced. These average soil characteristics are rated on a scale from 0 to 1, in which the lower values indicate higher erodibility. Tables A1-A3 illustrate these ratings: soils rich in clay (much coherence), with low bulk density (high water absorption) and which are deep (less danger of sliding over rocky sublayer) are least erodible and get index ratings of value 1.0. Soils with completely opposite characteristics get index ratings of value 0.6.

Table A1. Rating of soil texture index (I_t*)*

Index (I_t)	Textural class[1]
1.0	C, SC, SiC
0.8	S, LS, SCL, CL, SiCL
0.6	L, SL, Si, SiL

[1] Codes for textural class from USDA indicate C=clay, Si=silt, L=loam, S=sand. Peat soils are assigned an index 1.0 by default

*Table A2. Rating of the bulk density index (*Ib*)*

Index (I_b)	Bulk density ($kg.m^{-3}$)
1.0	b < 1350
0.8	1350 < b < 1550
0.6	b > 1550

*Table A3. Rating of the soil depth index (*Id*)*

Index (I_d)	Soil depth (cm)
1.0	d > 100
0.8	50 < d < 100
0.6	d < 50

The relief indicator is adapted from the 3 slope angle classes on the FAO Soil Map of the World (1991). Each depicted soil polygon has an assigned slope angle class (incorporated as an *a*, *b* or *c* in the soil identification code); soils on steep slopes are more vulnerable to erosion (Table A4).

Table A4. Rating of the slope angle index (I_a*)*

Index (I_a)	Slope angle class[1] (a in %)
1.0	a < 8
0.8	8 < a < 30
0.6	a > 30

[1] *FAO Soil Map of the World (FAO, 1991).*

A subrating for terrain erodibility (T_s), based on the soil and terrain characteristics, is calculated for each soil type *s* according to:

$$T_s = I_l \times I_o \tag{A3}$$

with: I_l - most limiting index of I_a, I_b, I_d and I_t.
I_O - average of the remaining 3 indices.

*Table A5. Rating of terrain erodibility (*T*)*

T-rating	Terrain erodibility (T_s)
1 – Low	Ts > 0.74
2 – Moderate	0.48 < T_S < 0.74
3 – High	T_S < 0.48

*Table A6. Example of terrain erodibility rating (*T*)*

Soil type[1]	I_t	I_b	I_d	I_a	T
Rx	0.6	0.6	0.8	0.8	0.4
Pf	0.8	1.0	1.0	0.8	0.8
Vp	1.0	0.6	1.0	1.0	0.6
Od	1.0	1.0	1.0	1.0	1.0
I	0.6	0.8	0.6	0.6	0.4

[1] R_x = gelic Regosols; P_f = ferric Podzols; V_p = pellic Vertisols; O_d = dystric Histosols; I = Lithosols.
[2] I_t: soil texture index; I_b: bulk density index; I_d: soil depth index; I_a: relief index (0.6 – most erodible; 1.0 least erodible).
[3] Terrain erodibility (0 - most erodible; 1.0 - least erodible).

The value of *T* can be classified according the class limits in Table A5 to distinguish between low, moderate and high erodibility. Since the calculation of *T* depends on the pre-classified values of the indicators with only three different values, T can assume only a limited number of discrete values (see examples in Table A6).

Rainfall erosivity (*R*)
The rainfall erosivity index *R* depends on rainfall intensity, amount and distribution. Detailed rainfall characteristics are not available on a global scale. Batjes (1996a) referred to De Pauw et al. (1996) and Bouwman (1989) for the approximation of rainfall erosivity, which method is primarily based on the annual precipitation amount and zonal rainfall characteristics (see Table A7).

*Table A7. Rating of the rainfall erosivity index (*R*)*

R-class	Rainfall erosivity
1 – Low	R < 800
2 – Moderate	800 < R < 1250
3 – High	1250 > R

Source: Major Agro-Ecological Zones map (De Pauw et al., 1996) and data from Bouwman (1989).

Land use pressure (*V*)
The land cover index *V* is the factor that is most directly influenced by human intervention. In the calculation method of Batjes (1996a) this factor determines the actual sensitivity by water erosion. This implies that changes in land cover through changes in management practices provide the most direct means for the abatement of erosion processes. Batjes (1996a) derived data on current land cover from Matthews (1983), see Table A8.

*Table A8. Rating of land cover index (*V*)*

V-class	Cultivation intensity[1] V_j (%)
1 – Well protected	0-19
2 – Moderately protected	20-49
3 – Poorly protected	50-100

[1] Cultivation intensity from Matthews (1983)

Susceptibility and sensitivity
The part of erosion risk that is due to the relatively 'constant' factors of climate and terrain is often termed 'potential' soil erosion (*Ep*), which describes the erosion expected when the terrain is not protected by vegetation. Batjes (1996a) prefers the term susceptibility as this kind of erosion rating refers to a hypothetical situation:

Table A9. Rating of the susceptibility to water erosion

Susceptibility (*Ep*)	Rainfall erosivity (*R*)	Terrain erodibility (*T*)
1 – Low	1 or 2	1
2 – Moderate	Any other combination	Any other combination
3 – High	2 or 3	2 or 3

In addition, Batjes (1996a) assigned the term sensitivity to the (presumed) risk of soil types being affected by water erosion under current conditions of land cover: the actual erosion risk (*Ea*). Sensitivity combines rainfall erosivity, terrain erodibility and land cover:

Table A10. Rating of the sensitivity to water erosion.

Sensitivity (*Ea*)	Rainfall erosivity (*R*)	Terrain erodibility (*T*)	Land cover (*V*)
1 – Low	1	1	1
	<3	1	1
	1	<3	1
2 – Moderate	Any other combination	Any other combination	Any other combination
3 – High	>2	>2	>2
	3	1	3

Mailing list

1. D.C. de Bruijn, VROM - DGM/IMZ
2. Y. de Boer, VROM, DGM/IMZ
3. T. Zwartepoorte, VROM DGM/LE
4. J. Broerse, BZ, DML
5. M Chenje, UNEP, Kenya
6. M Chenje, UNEP, Kenya
7. M Chenje, UNEP, Kenya
8. D. Claasen, UNEP, Kenya
9. M. Cheatle, UNEP, Kenya

10-65 UNEP Collaborating Centers

66. J. Alcamo, University of Kassel
67. N.H. Batjes, ISRIC, Wageningen
68. J. Bruinsma, FAO, Rome
69. R. Darwin, USDA, Washington, D.C.
70. J. Dumanski, Ottawa, Canada
71. V.W.P. van Engelen, ISRIC, Wageningen
72. A.R. Gentile, EEA, Copenhagen
73. S. Nixon, WRC, Medmenham, U.K.
74. L.R. Oldeman, ISRIC, Wageningen
75. C. Pieri, Worldbank, Washington, D.C.
76. M.W. Rosegrant, IFPRI, Washington, D.C.
77. C. Russel, WRC, Medmenham, U.K.
78. M. Schomaker, Lentilleres, France
79. J. Tschirley, FAO, Rome
80. V. Vandeweerd, UNEP, The Hague
81. M. Winograd, CIAT, Cali, Colombia
82. N.D. van Egmond
83. F. Langeweg
84. R. van den Berg
85. A.H.M. Bresser
86. A.W. van der Giessen
87. J.A. Hoekstra
88. D. van Lith
89. R.J.M. Maas
90. G.J. Heij
91. J.A. Bakkes
92. G.J. van den Born
93. L. Brandes
94. H. Bronswijk
95. K. Buurman
96. B. de Vries
97. B. Eickhout
98. C.G.M. Klein Goldewijk
99. B. Metz
100. J. Van Minnen
101. A. de Moor
102. M. Schaeffer
103. B. Strengers
104. K. Wieringa
105. J. Wiertz
106. J.W. van Woerden
107. Bureau Rapportenregistratie
108. SBD/Voorlichting & Public Relations
109. Bibliotheek RIVM

105-113 Auteurs
114-134 Bureau Rapportenbeheer
135 Depôt Nederlandse Publikaties en Nederlandse Bibliografie